PERGAMON

International Journal of Heat and Mass Transfer 43 (2000) 4135–4151

International Journal of HEAT and MASS TRANSFER

www.elsevier.com/locate/ijhmt

Reaction–diffusion model of surface and grain boundary segregation kinetics

T. Gambaryan-Roisman, E. Litovsky, M. Shapiro*, A. Shavit

Laboratory of Transport Processes in Porous Materials, Faculty of Mechanical Engineering, Technion–Israel Institute of Technology, Haifa 32000, Israel

Received 9 February 1999; received in revised form 10 January 2000

Abstract

Small amounts of impurities normally present within crystalline solid materials tend to segregate near the surfaces of pores. A mathematical model for the surface segregation kinetics is proposed. An analytical solution is obtained for the evolution of the impurity's surface concentration, induced by an instantaneous change of the material's temperature. For times, significantly exceeding the characteristic diffusion time, when the segregation process is controlled by the bulk diffusion, the segregation kinetic curve reduces to the McLean's expression. For times, which are short compared to the reaction time, segregation is shown to be entirely controlled by the surface reaction kinetics. The effect of the grain boundary parameters on the segregation of impurities on surfaces of small pores is studied. The analyses are performed for grains and pores of plane, cylindrical and spherical shapes. The results calculated for surface segregation kinetics are fitted with experimental data for segregation of silver in copper and sulfur in Fe–6at.%Si, available from the literature. This allowed calculation of the surface reaction constant and the segregation length, appearing in the model. These quantities showed the Arrhenius temperature dependence. © 2000 Published by Elsevier Science Ltd.

1. Introduction

Surface and grain boundary segregation processes affect mechanical, electrical and thermophysical properties of metals and ceramic materials [1,2]. The segregation of impurities in the grain boundary regions of ceramic and composite materials affects their transport properties, in particular, the diffusivity of impurities atoms, electrical and thermal conductivity [3]. When the temperature of a ceramic specimen is changed, the concentration C_s of a segregated substance on surfaces of small pores prevailing in the grain boundary region changes very slowly, long time after a thermal equilibrium has been established. This slow mass redistribution process brings about a comparable temporal change of the thermal conductivity in vacuum [4]. In order to rationalize such a behavior of thermophysical properties of ceramic materials, a physico-mathematical model of surface segregation kinetics on small pores is needed.

Different models for surface segregation kinetics have been proposed in the literature [5,6]. The rate of segregation of impurities on a surface of a crystal grain/pore is controlled by two processes: (i) surface reaction, governing the exchange rate between the bulk and the surface regions; (ii) bulk diffusion

* Corresponding author. Tel.: +972-48-293-185; fax: +972-48-324-533.

E-mail address: mersm01@techunix.technion.ac.il (M. Shapiro).

0017-9310/00/$ - see front matter © 2000 Published by Elsevier Science Ltd.
PII: S0017-9310(00)00034-X

Nomenclature

a	pore size
$\bar{a} = a/\gamma\delta$	nondimensional pore size
b	thickness of the near surface region
$\bar{b} = b/\delta_*$	parameter
$\hat{c}(\bar{x}, s)$, $\hat{c}(\bar{r}, s)$, $\hat{c}_s(s)$	Laplace transforms of the concentrations
$c_s = \frac{C_s - C_{si}}{C_{s0} - C_{si}}$	nondimensional surface concentration
$c = \frac{C - C_\infty}{C_{s0} - C_{si}}$	nondimensional bulk concentration
C	concentration of the impurities in the bulk phase
C_s	concentration of a segregated substance on surfaces
C_∞	bulk concentration of impurities far from the surface
C_s^{eq}	equilibrium surface coverage
C^{eq}	equilibrium surface concentration
C_{si}	initial surface coverage
C_{s0}	surface concentration derived from Eq. (11)
$C_i = C^{\mathrm{eq}}(C_{si}, T)$	bulk concentration
D	bulk diffusivity coefficient
E_{segr}	segregation energy
D_{ns}	diffusion coefficient in the near surface region
I_0 and I_1	modified Bessel functions of the first kind
K_0	characteristic value of K (at large temperatures)
K_0 and K_1	modified Bessel functions of the second kind
K	surface reaction coefficient
L	characteristic size of the solid body
$\bar{L} = L/\gamma\delta$	nondimensional size of the solid body
$n = 1, 2, 3$	dimensionality parameter
$\mathbf{n}$	unit normal vector directed towards the bulk
p_1, p_2	parameters, see Eq. (23)
$\bar{r} = \frac{r}{\delta_*}$,	nondimensional coordinate
$\bar{x} = \frac{x}{\delta_*} = \frac{x}{\gamma\delta}$	nondimensional coordinate
$t_{\mathrm{segr}} = \delta_*^2/D$	characteristic segregation time
Q_K	characteristic energy governing temperature dependence of K
R	gas constant
s	Laplace variable
t	time
T	absolute temperature
w	function, see Eq. (24)
x, r	coordinates measured from the surface

Greek symbols

α	enrichment factor
β	reaction rate for two-dimensional growth
γ	differential enrichment coefficient
γ_1	parameter, see Eq. (37)
δ	layer thickness,
$\delta_* = \gamma\delta$	length scale of segregation
δ_{*0}	characteristic segregation thickness
$\sigma = \sqrt{D/D_{\mathrm{ns}}}$	parameter
κ	reaction rate constant
$\mu = D/K\delta_*$	surface Damköhler group
$\tau = \frac{t}{t_{\mathrm{segr}}} = \frac{tD}{\delta_*^2}$	nondimensional time
$\varphi(s)$	function, see Eq. (A3)

of impurities, which determines the rate at which the inhomogeneous volumetric concentration distribution is transported in the bulk.

McLean [1,6] has proposed a model for surface segregation kinetics, in which bulk diffusion was assumed to be the only mechanism, controlling the rate of segregation–desegregation of impurities. This model is based on the solution of the diffusion equation within a semi-infinite region subject to the condition of mass conservation at the surface. A linear relationship was assumed between the surface concentration, C_s, and the "near-surface" volumetric concentration, $C|_{x=0}$ (Fig. 1a). As a result, the following expression for the surface concentration was obtained for zero initial surface concentration [6]:

$$C_s(t) = \alpha C_\infty \left[1 - \exp\left(\frac{Dt}{\alpha^2\delta^2}\right)\mathrm{erfc}\left(\frac{Dt}{\alpha^2\delta^2}\right)^{1/2} \right], \qquad (1)$$

where δ is the surface layer thickness, D is the bulk diffusivity coefficient, C_∞ is the bulk concentration of impurities far from the surface, and the "enrichment factor" α is the ratio between the equilibrium surface concentration and the bulk concentration of impurities.

However, numerous experimental data could not be fitted by McLean's expression (1) [7,6]. This suggests that McLean's model is oversimplified. The source of

oversimplification is the assumption that no resistance to the bulk-surface flux of segregated substance is exerted by the surface.

In the case of very strong segregation, Crank's solution [8] can be employed for describing the segregation kinetics [6,9]. This model is based on the diffusion equation in semi-infinite space, subject to mass conservation condition at the surface and condition of ideal sink near the surface: $C(x=0)=0$. As a result one obtains the following time dependence of the surface concentration of impurities:

$$C_s(t) = \frac{2}{\delta} C_\infty \left(\frac{Dt}{\pi}\right)^{1/2}. \tag{2}$$

This expression can be derived from the McLean formula (1) at $t \ll \alpha^2\delta^2/D$, and is valid for low surface coverage.

McLean's model is based on a linear relationship between the surface and near-surface impurities' concentrations. Rowlands and Woodruf [10] attempted to improve this model by expressing the condition of local equilibrium between the surface and near-surface layer in the form of a generally nonlinear segregation isotherm. However, both McLean's model and the model of Rowlands and Woodruf are not valid in cases, where segregation is governed by the kinetics of the surface reaction. As such, both models do not account for the surface reaction rate.

The surface reaction rate has been accounted for in reaction-rate limited models [11–13,6]. A first-order reaction has been proposed at the surface, i.e. the rate of change of the surface concentration of impurities is proportional to the difference between the equilibrium and the current surface concentration. As a result, the following expression for evolution of surface concentration was obtained [6]:

$$C_s(t) = \alpha C(1 - e^{-\kappa t}), \tag{3}$$

where κ is the reaction rate constant and αC is the saturation concentration. This approach describes physical situations where surface concentration kinetics is controlled by the reaction rate. It is a case for certain class of solid solutions, for example, for carbon dissolved in tungsten [11,6], where the bulk diffusion of solute atoms is more rapid than the migration of solute atoms from the bulk phase into the surface. This migration is determined by the rate at which the atoms pass through the surface. Such reaction-rate limited model cannot adequately describe physical situations, where bulk diffusion affects the segregation process.

A generalized model for segregation kinetics is needed, which accounts for both the bulk diffusion and the surface reaction mechanisms and can adequately describe the cases, where these two mechanisms coexist. Such a model was developed by du Plessis and van Wyk [14], du Plessis [6]. It accounts for the bulk diffusion, as well as for the surface resistance (energy barrier) to migration of impurities' atoms from the bulk to the surface. In this model, a semi-infinite region is divided into layers of equal size, the first of which was related to the surface, and all others were related to the bulk. The mass flux between two adjacent layers was assumed to be proportional to the difference between impurities' chemical potentials prevailing at these layers, to the concentration of species and their mobility. The rate equation for impurities' concentration was formulated for each layer, and the resulting system of ordinary differential equations was solved numerically.

Our work is motivated by the analysis of heat trans-

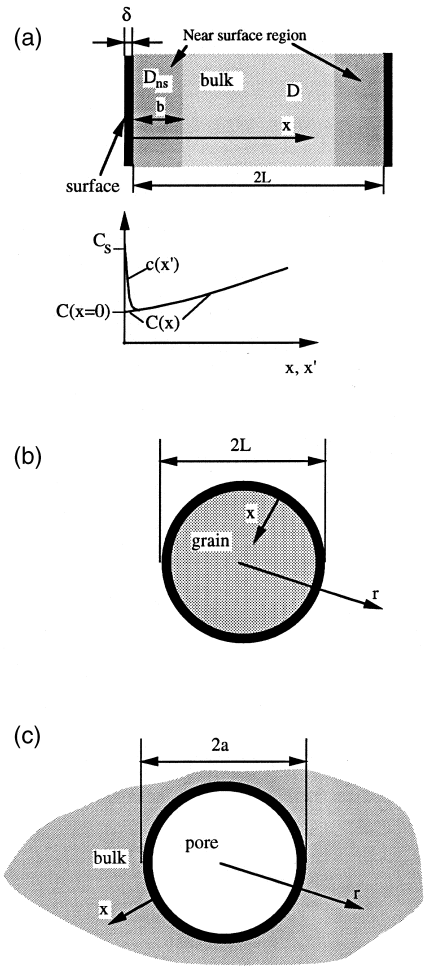

Fig. 1. (a) Plane geometry for segregation kinetics modeling. (b) Model for cylindrical or spherical grain. (c) Model of cylindrical or spherical pore.

fer in porous ceramic materials, characterized by complex geometric structures and existence of small pores. Thermophysical properties of porous ceramics depend upon the segregation of impurities to the surfaces of small pores, present at the grain boundaries [15,3,4]. The application of du Plessis' method for such systems leads to computational difficulties, especially for a complex microstructure, characteristic of oxide ceramic materials.

Other models for segregation kinetics which are relevant to this work include the models of Kristyan and Giber [16], du Plessis et al. [16,17], and Bezuidenhout et al. [19]. They possess limited ranges of applicability. Bezuidenhout et al. [19] pointed out that neither of the above kinetic equations (Eqs. (1)–(3)) satisfactorily correlate the experimental data collected on segregation of carbon to (110) surface of a Fe–10at.%Si single crystal. In their study they tried to fit the data by a model accounting to island formation [20] by means of the equation

$$C_s(t) = C_s^{\mathrm{eq}}\left[1 - \exp\left(-\frac{1}{2}\beta t^2\right)\right], \tag{4}$$

where C_s^{eq} the equilibrium surface coverage and β is the reaction rate for two-dimensional growth.

Several works have been devoted to kinetics of weak surface segregation [16–18], which is defined as surface segregation in systems characterized by low enrichment factors. Only discrete (discontinuous) models requiring numerical methods were proposed for this situation.

In this study, we propose an analytical linear model for the surface segregation process. The specific goals are investigation of (i) the segregation process on the surfaces of micro and nanopores and (ii) the influence of the pore surface curvature and the material's grain size on the segregation kinetics. Analytical solutions are helpful for investigation of limiting cases, i.e. reaction- and diffusion-controlled segregation regimes, and also for determination of the applicability limits of the existing analytical expressions. In the following section, a linear model of segregation kinetics is developed and used to obtain analytical expressions, describing temporal evolution of C_s, caused by a sudden change of thermodynamic conditions. This model accounts both for the bulk diffusion and surface reaction mechanisms of segregation kinetics and allows application to various grains and pore geometries.

2. Segregation kinetics analysis based on the reaction–diffusion model

In our analysis the material will be assumed to consist of two phases: bulk and surface. The concentration of the impurities in the bulk phase, C, can vary with the spatial coordinate x or r and the time, t, and the surface concentration of impurities, C_s, is a function of time only. The simplest geometric system is the semi-infinite space (bulk), limited by a plane surface ($b = 0$, $L = \infty$ in Fig. 1a). In order to describe the kinetics of impurities' segregation on the boundary of a single grain, we shall use the following models: (i) slab bounded by two infinite parallel surfaces separated by a distance $2L$ (Fig. 1a with $b = 0$, finite L), (ii) cylinder or sphere of radius L (Fig. 1b). The analysis of segregation of impurities at the individual pore's surface will be performed with the help of cylindrical and spherical pores models (Fig. 1c). When studying the grain boundary segregation, it is important to account for the diffusion in the near-surface region, which can be significantly faster or in some cases slower [16] than the bulk diffusion of impurities [2]. For this purpose, a third phase, or near-surface region of a thickness b can be included, possessing a diffusion coefficient $D_{\mathrm{ns}} \neq D$ (Fig. 1a, $b > 0$).

The bulk concentration of the impurities in the bulk region is governed by the diffusion equation:

$$\frac{\partial C}{\partial t} = D\nabla^2 C \tag{5}$$

The equation of mass conservation at the surface can be written as follows:

$$\delta\frac{\mathrm{d}C_s}{\mathrm{d}t} = D\,\mathbf{n}\cdot\nabla C, \tag{6}$$

where $\mathbf{n}$ is the unit normal vector directed towards the bulk.

Implicit in the above equations is the assumption that the bulk variable x (appearing in Eq. (5)) is viewed at a length scale L, greatly exceeding the thickness δ of the surface layer. Therefore, the bulk concentration $C(x)$ is determined using the lengthscale L everywhere, even at the pore surface $x = 0$ (see Fig. 1a). In contrast with this, a microscale concentration, at the scale δ may be independently defined [21], i.e., $c(x')$, where x' is the spatial coordinate measured at the micro-length scale δ. These concentrations are equal everywhere except in the region δ adjacent to the pore surface (see Fig. 1a). The limiting value of c at $x' \to 0$ serves as a formal definition of the surface concentration C_s, i.e., $c(x' \to 0) = C_s$. It clearly differs from the "outer" limit $C(x \to 0)$, which defines the value of the bulk concentration on the pore-surface $C(x = 0) \neq C_s$. Note also that for very thin surface layer δ, a reduced surface concentration C_s' (per unit area) is frequently defined [22]) as $C_s' = \delta C_s$. For the sake of clarity and comparison with different models, we will nevertheless use the "volumetrically defined" concentration at the surface region, C_s.

To formulate an additional boundary condition, we

assume that the impurities flux from the bulk layer adjacent to the surface to the surface itself is governed by the local equilibrium between the instantaneous surface and bulk concentrations of impurities. That is, the rate of change of the surface concentration is proportional to the difference between the instantaneous concentration in the bulk adjacent to the surface, $C|_{x=0}$, and the bulk concentration prevailing at equilibrium with the instantaneous surface concentration C_s at the current temperature T, i.e. $C^{\mathrm{eq}}(C_s, T)$:

$$\frac{\mathrm{d}C_s}{\mathrm{d}t} = \delta^{-1}K\left\{(C)_{x=0} - C^{\mathrm{eq}}(C_s, T)\right\}, \tag{7}$$

where C is the bulk concentration of impurities, t is the time variable, and x is the coordinate in the direction normal to the surface. The factor K is the surface reaction coefficient, which can be related to the 'reaction rate' κ (Eq. (3)), and to the bulk-surface mobility of impurities [6]. This factor may depend upon the surface orientation with respect to crystal lattice axes and can constitute one of the factors, leading to the difference between the segregation rates to differently oriented surfaces in the cases, where the segregation kinetics is partly reaction controlled [9,23]. The function $C^{\mathrm{eq}}(C_s, T)$ can be derived from the segregation equation, for example, Bragg–Williams equation or McLean's equation [1,6].

Eqs. (5)–(7) are to be solved for the bulk concentration field $C(x, t)$ and the surface concentration history $C_s(t)$ subject to the initial conditions

$$C(x, 0) = C_\infty \tag{8}$$

and

$$C_s(0) = C_{si}, \tag{9}$$

where C_∞ is the bulk concentration infinitely far from the surface, C_{si} is the initial surface coverage.

To facilitate the solution we will linearize the functional dependence $C^{\mathrm{eq}}(C_s, T)$ approximated in the following form:

$$C^{\mathrm{eq}}_{\mathrm{appr}} = C + \frac{C_s - C_{s0}}{\gamma}, \tag{10}$$

where C_{s0} is derived from

$$C_\infty = C^{\mathrm{eq}}(C_{s0}, T), \tag{11}$$

$$\frac{1}{\gamma} = \left(\frac{\partial C^{\mathrm{eq}}}{\partial C_s}\right)_{C_{s0},\, T}. \tag{12}$$

The last parameter, which can be called "differential enrichment coefficient", obviously depends on the specific type of segregation isotherm, pertaining to the given system. For example, for the Langmuir–McLean isotherm

$$\gamma = \frac{\exp\left(E_{\mathrm{segr}}/RT\right)}{\left[1 + C_\infty \exp\left(E_{\mathrm{segr}}/RT\right)\right]^2}$$

$$= \exp\left(\frac{E_{\mathrm{segr}}}{RT}\right)\left[1 - C_{s0} + C_{s0}\exp\left(-\frac{E_{\mathrm{segr}}}{RT}\right)\right]^2, \tag{13}$$

where E_{segr} is the segregation energy and R is the gas constant. The Bragg–Williams segregation isotherm [6] yields a more complicated expression for γ. Utilizing the multilayer approach, based on the tight-binding Ising model, allows the calculation of the equilibrium segregation isotherm by solution of system of simultaneous equations [24], in which case γ can be evaluated numerically. In the case of multicomponent alloys, γ depends also on concentration of other impurities and on their modes of interaction [25]. This parameter may also depend on the surface orientation [26]. Generally, γ is less than α by a factor $[1 - C + C\exp(E_{\mathrm{segr}}/RT)]$. However, for small C and $C\exp(E_{\mathrm{segr}}/RT)$ these parameters have close values.

Linearization (10) is valid for small changes of C_s. The limits of applicability of Eq. (10) are discussed in Section 4.

Eqs. (5)–(12) constitute a well-posed problem that can be formulated for any geometry. For simple geometries of a semi-infinite plate, cylinder and sphere, closed form solutions can be obtained by the Laplace transform method (see Appendix A).

It must be noted that the model of semi-infinite space is a limiting case for the models of planar, cylindrical or spherical grain in the limit $\bar{L} = L/\gamma\delta \to \infty$, and also for the model of cylindrical or spherical pore in the limit $\bar{a} = a/\gamma\delta \to \infty$.

Our model does not use the assumption of the local equilibrium between the bulk and surface concentrations of impurities. We assume that the surface resists to the free bulk-surface motion of the species, necessary for establishment of this equilibrium. This resistance is quantified by the surface reaction coefficient K via Eq. (7).

Below, an analytical treatment for the plane semi-infinite slab model will be presented followed by a comparison with the finite grain and pore models.

The following nondimensional variables are introduced:

$$\bar{x} = \frac{x}{\delta_*} = \frac{x}{\gamma\delta}, \quad \bar{r} = \frac{r}{\delta_*}, \quad \tau = \frac{t}{t_{\mathrm{segr}}} = \frac{tD}{\delta_*^2}, \tag{14a,b,c}$$

$$c_s = \frac{C_s - C_{si}}{C_{s0} - C_{si}}, \qquad c = \frac{C - C_\infty}{C_{s0} - C_{si}}, \tag{15a,b}$$

where x is the spatial variable in the planar geometry,

r is the spatial variable in the spherical case, $\delta_* = \gamma\delta$ is the characteristic length scale of segregation.

In terms of these new variables, the problem posed for the semi-infinite space adopts the form:

$$\frac{\partial c}{\partial \tau} = \frac{\partial^2 c}{\partial \bar{x}^2}, \quad \tau \geq 0, \bar{x} \geq 0, \tag{16}$$

$$\frac{\mathrm{d}c_s}{\mathrm{d}\tau} = \gamma \frac{\partial c}{\partial \bar{x}}, \quad \tau > 0, \bar{x} = 0, \tag{17}$$

$$\mu \frac{\mathrm{d}c_s}{\mathrm{d}\tau} = (c\gamma - c_s + 1), \quad \tau > 0, \bar{x} = 0, \tag{18}$$

$$c = 0, \quad c_s = 0, \qquad \tau = 0, \quad \bar{x} \geq 0, \tag{19a,b}$$

where the parameter

$$\frac{1}{\mu} = \frac{K\delta_*}{D} \tag{20}$$

characterizes the relation between the surface reaction and bulk diffusion rates, and can be interpreted as a surface Damköhler group.

Eqs. (16)–(19) were solved by the Laplace transform method. The following expressions for the evolution of bulk and surface impurities' concentration were obtained:

$$c = -\frac{1}{\gamma\sqrt{1-4\mu}} \exp\left(-\frac{\bar{x}^2}{4\tau}\right)\left[w\left(p_1\sqrt{\tau} + \frac{\bar{x}}{2\sqrt{\tau}}\right) - w\left(p_2\sqrt{\tau} + \frac{\bar{x}}{2\sqrt{\tau}}\right)\right], \tag{21}$$

$$c_s = 1 - \frac{1}{\sqrt{1-4\mu}}\left[\frac{w(p_1\sqrt{\tau})}{p_1} - \frac{w(p_2\sqrt{\tau})}{p_2}\right], \tag{22}$$

where

$$p_1 = \frac{(1-\sqrt{1-4\mu})}{2\mu}, \qquad p_2 = \frac{(1+\sqrt{1-4\mu})}{2\mu}, \tag{23}$$

$$w(z) = \exp(z^2)\mathrm{erfc}(z). \tag{24}$$

If $\mu \gg 1$, the segregation kinetics is reaction controlled, and Eq. (22) reduces to

$$c_s = 1 - \exp(-\tau/\mu) = 1 - \exp(-tK/\delta_*), \tag{25}$$

which is identical to Eq. (3) with $\kappa = K/\delta_*$. If, on the contrary, $\mu \ll 1$, the process is controlled by the bulk diffusion, and Eq. (22) reduces to

$$c_s = 1 - \exp(\tau)\mathrm{erfc}(\tau^{1/2}) = 1 - \exp(tD/\gamma^2\delta^2)\mathrm{erfc}(tD/\gamma^2\delta^2)^{1/2}, \tag{26}$$

which resembles Eq. (1) with enrichment ratio α substituted by γ. These two expressions become identical when $\alpha = \gamma$, i.e. when the equilibrium value of C_s depends linearly on C.

When $\mu \sim 1$, neither of these mechanisms dominates during the entire process. Attention will now be focused at the asymptotic behavior of the surface segregation kinetics. For short times ($\tau \ll \mu$ or $t \ll \delta_*/K$) Eq. (22) simplifies to Eq. (25), which points out at the limiting role of the surface reaction on the segregation kinetics. For long times ($\tau \gg 1$, $\tau \gg \delta_*^2/D$) the asymptotic behavior of Eq. (22) is described by Eq. (26). It can be concluded that at the final stage of the segregation process the bulk diffusion rate plays the limiting role.

Our reaction–diffusion model for segregation kinetics includes the results of McLean's and Rawlings–du Plessis' models as asymptotics valid for diffusion-controlled and reaction-controlled cases, respectively.

In order to determine the applicability range of the hypothesis of infinite source of impurities for description of the grain boundary segregation in ceramic materials, we shall analyze the segregation of impurities on the edges of the slab (Fig. 1a, finite L) and on the surfaces of the cylinder and sphere (Fig. 1b).

The ultimate values of bulk and surface concentrations of impurities $C(x, t\to\infty) \neq C_\infty$ and $C_s(t\to\infty) \neq C_{s0}$ can be found from the solution of the following system of equations written for a slab:

$$C(x, t\to\infty) = C + \frac{C_s(t\to\infty) - C_{s0}}{\gamma}, \tag{27}$$

$$2LC(x, t\to\infty) + 2\delta C_s(t\to\infty) = 2LC + 2\delta C_{si}. \tag{28}$$

Eq. (27) expresses the fact that at $t\to\infty$, the equilibrium between the bulk and surface concentrations of impurities at temperature T is reached. Eq. (28) expresses conservation of impurities in the chosen volume. These equations can be solved to yield:

$$C(x, t\to\infty) = C + \frac{C_{si} - C_{s0}}{\gamma(n + \bar{L})}, \tag{29}$$

$$C_s(t\to\infty) = C_{si} + \frac{C_{s0} - C_{si}}{1 + n/\bar{L}}, \tag{30}$$

where $n = 1, 2, 3$ for parallel plate, cylindrical and spherical grains, respectively and $\bar{L} = L/\delta_*$.

One can see that, generally, the bulk concentration level decreases as a result of segregation ($C_{s0} > C_{si}$,

because the impurities are pumped out of the bulk onto the surface, and increases as a result of desegregation. Moreover, $C_{si} < C_s(t\to\infty) < C_{s0}$ in the case of segregation, and $C_{si} > C_s(t\to\infty) > C_{s0}$ for desegregation. For large grains ($\bar{L} \gg 1$) the bulk concentration retains its initial value and C_s reaches C_{s0}, in accordance with the case of an "infinite" grain. In the opposite case ($\bar{L} \ll 1$), the bulk concentration changes dramatically, and the surface concentration changes only slightly.

For the analysis of the impurities' segregation on the surface of a plate possessing finite width, Eq. (5) must be solved in the domain $-\bar{L} < \bar{x} < \bar{L}$ for slab or $0 < \bar{r} < \bar{L}$ for cylindrical or spherical grain subject to boundary and initial conditions (17)–(19). This equation was solved by the Laplace transform's method. The solution is given in Appendix A and shown in Fig. 5.

We further study the kinetics of surface segregation on the surfaces of small pores existing in the grain boundary region [3]. Towards this goal, Eq. (5) subject to conditions (17)–(19) is solved in the domain $\infty > \bar{r} > \bar{a} = a/\delta_*$ for cylindrical or spherical pores. These solutions are presented in Appendix A and illustrated in Fig. 6. Their discussion is presented in Section 3.

In order to analyze the influence of the near-surface region thickness b and $D_{\rm ns}$ on the surface segregation kinetics, a three-layer model is considered (Fig. 1, finite L). The first layer is the surface layer of the width δ, the second layer is adjacent to the first and called "near-surface region" (b, $D_{\rm ns}$), and the third is the bulk region, where the impurities have diffusivity D. The set of governing equations and boundary conditions are modified appropriately.

Eq. (5) must be solved successively in the bulk and near-surface regions with respective diffusivities D and $D_{\rm ns}$, subject to the conditions of continuity of the concentration and its flux at $x = b$.

The resulting solution is governed by the dimensionless parameters

$$\sigma = \sqrt{D/D_{\rm ns}}, \qquad \bar{b} = b/\delta_* \tag{31}$$

and is presented in Appendix A. If $\sigma = 1$ or $\bar{b} = 0$, the present solution reduces to the regular planar case, described by Eqs. (22)–(24).

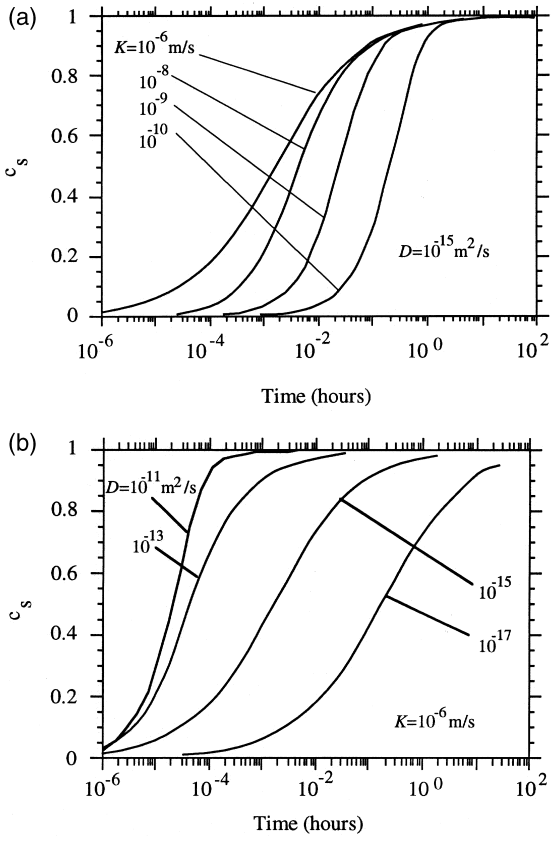

Fig. 2. Influence of reaction (a) and diffusion (b) coefficients on the segregation kinetics.

3. Results

The time dependence of C_s for the simplest case (semi-infinite space) is shown in Fig. 2a and b, where the effects of D and K on C_s are shown. Fig. 2a exhibits the influence of the surface reaction coefficient K on the segregation kinetics. At the final stage of the segregation, $C_s(t)$ does not depend upon K. However, K determines the enrichment rate at the onset of the segregation process.

Fig. 2b depicts the influence of the bulk diffusion coefficient D on the segregation process with all other parameters fixed. One can see that at the early stage of the segregation process, C_s is nearly unaffected by the diffusion coefficient. However, at the final stage of the segregation this coefficient determines the duration of the segregation process. Namely, when the diffusion coefficient is small (for example, at low temperatures), the segregation process occurs slowly. In the conditions of a relatively fast cooling of a specimen to a lower temperature the surface concentration remains effectively frozen. Duration of the segregation process decreases in the inverse proportion to D, while $D \ll K\delta_*$. With increasing D, the segregation curve approaches the exponential form (3) with $\kappa = K/\delta_*$.

The nondimensional complex μ determines the relationship between the bulk diffusion and the surface reaction rate and, therefore, governs the surface segregation kinetics, which is graphically illustrated in Fig. 3.

Variation of surface concentration with dimensionless time τ for various values of μ is shown in Fig. 3. One can see that for $\mu = 0.1$ the $c_s(\tau)$ curve is very close to that described by the pure diffusion limited model (Fig. 3a). When $\mu < 0.1$, the process is diffusion-limited and can be described by Eq. (26). As μ increases, the $c_s(\tau)$ curve deviates from the diffusion-limited behavior. For $\mu \sim 1$ both mechanisms (diffusion and reaction) are equally important (Fig. 3b). For $\mu = 10$ the segregation–diffusion curve is very close to that described by the reaction model (Fig. 3c). If $\mu > 10$, then the surface reaction limits the rate of the segregation process, and surface segregation is described by Eq. (25). For intermediate values of μ, the general reaction–diffusion model of the segregation kinetics must be applied. Therefore, the ranges of applicability of the McLean and reaction (Rawlings–du Plessis) models are established in terms of the parameter μ.

Fig. 4 depicts the evolution of bulk concentration distribution calculated via Eq. (21) for $\mu = 0.1$–100. Fig. 4a exhibits a distribution of dimensionless bulk concentration $\gamma(C - C)/(C_{si} - C_{s0})$ at several time instants for $\mu = 1$. At the early stage of the segregation process the deviation of the bulk concentration from C is significant only in the immediate vicinity of the surface. This deviation monotonously increases and continuously propagates to the deeper layers of the material. This stage is characterized by very steep concentration gradients at the points adjacent to the surface. After reaching its maximum (see curve $\tau = 1.0$) in the immediate vicinity of the surface the dimensionless bulk concentration begins to decrease in this near-surface region. This new stage is characterized by "dissolution" of bulk concentration nonuniformity in the material.

Fig. 4b depicts the evolution of concentration at the point adjacent to the surface for various μ. It can be seen that the maximal difference between this concentration and that prevailing far from the surface occurs approximately at $\tau = \mu$, and the absolute value of this difference decreases with increasing μ.

Fig. 4c shows a comparison between the concentration profiles calculated by the reaction–diffusion model with $\mu = 10^{-4}$ (diffusion-controlled case) and

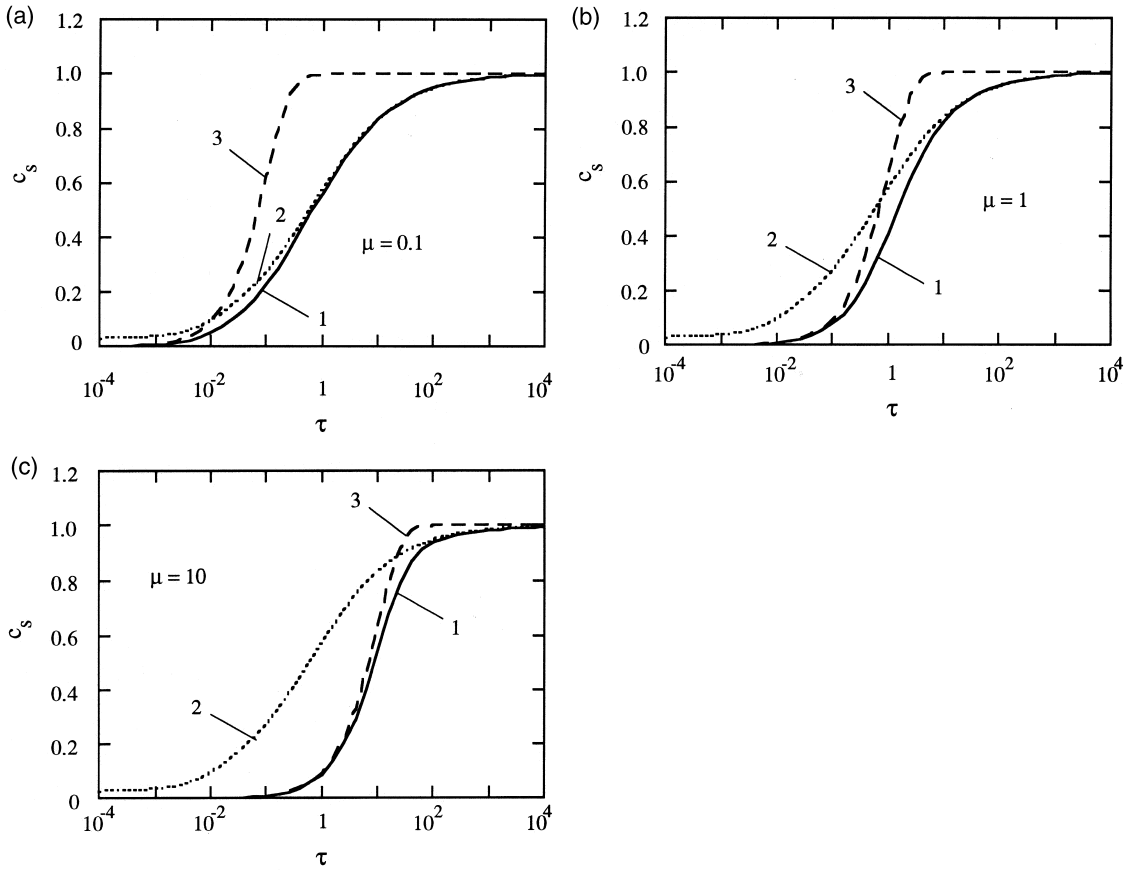

Fig. 3. Comparison of reaction–diffusion model with pure diffusion and pure reaction limits. (1) Reaction–diffusion model; (2) diffusion model (Eq. (26)); (3) reaction model (Eq. (25)). (a) $\mu = 0.1$; (b) $\mu = 1$; (c) $\mu = 10$.

the results of Crank's solution for the bulk concentration of impurities

$$C = C_\infty \operatorname{erf}\left(\frac{x}{2\sqrt{Dt}}\right), \tag{32}$$

derived under the assumption of a pure sink at the surface: $C(x=0)=0$. For comparison purposes it was assumed that $C_{si}=0$ and that $\alpha=\gamma$ (which is true for small $C_\infty \exp(E_{\text{segr}}/RT)$. One can see that these two models bring to very close concentration profiles at $\tau = 10^{-4}$, corresponding to extremum value of $C(x=0)$ curve. For dimensionless times significantly differing from 10^{-4}, C given by our model deviates from that of Crank's solution.

Fig. 4d compares the concentration profiles calculated by the reaction–diffusion model with $\mu = 0.1$ (kinetics is partly reaction-controlled) with Crank's solution. It is seen that in these conditions these two models yield different concentration profiles for all times. However, the values of the "depth of influence" of the segregation process as predicted by both models are similar.

Fig. 4a, c and d show that only a layer of thickness of the order δ_*, adjacent to the surface, is significantly affected by the segregation process. Consider now Fig. 5, which illustrates the influence of the nondimensional grain size $\bar{L}$ on the behavior of the segregation curve. At short times $\bar{L}$ does not influence the segregation process. The influence of $\bar{L}$ becomes important at later stages, when deeper material layers become involved in the segregation process. If $\bar{L} \sim \delta_*$, or $\bar{L} \sim 1$, the impurities from the whole grain are set in motion due to the segregation process. As a result, the C_s vs. t curve becomes sensitive to the limited quantity of the impurities present in the grain. In the case of small $\bar{L}$ the final bulk concentration of impurities decreases, and the equilibrium surface concentration decreases accordingly. However, if $\bar{L}$ exceeds 10, major part of the grain does not take part in the segregation process. In this case the solution for the finite grain reduces to the curve obtained for the semi-infinite space. For $\bar{L} > 10$ the assumption of the infinite source of impurities is rather satisfactory, and the material is effectively infinite. The same comments are applicable to the spherical grain also (Fig. 5c). However, in this case the effect of size is stronger due to the fact that the specific area of the sphere of diameter $2\bar{L}$, equal to $3/\bar{L}$, is more than the specific area of the slab of thickness $2\bar{L}$, which is equal to $1/\bar{L}$.

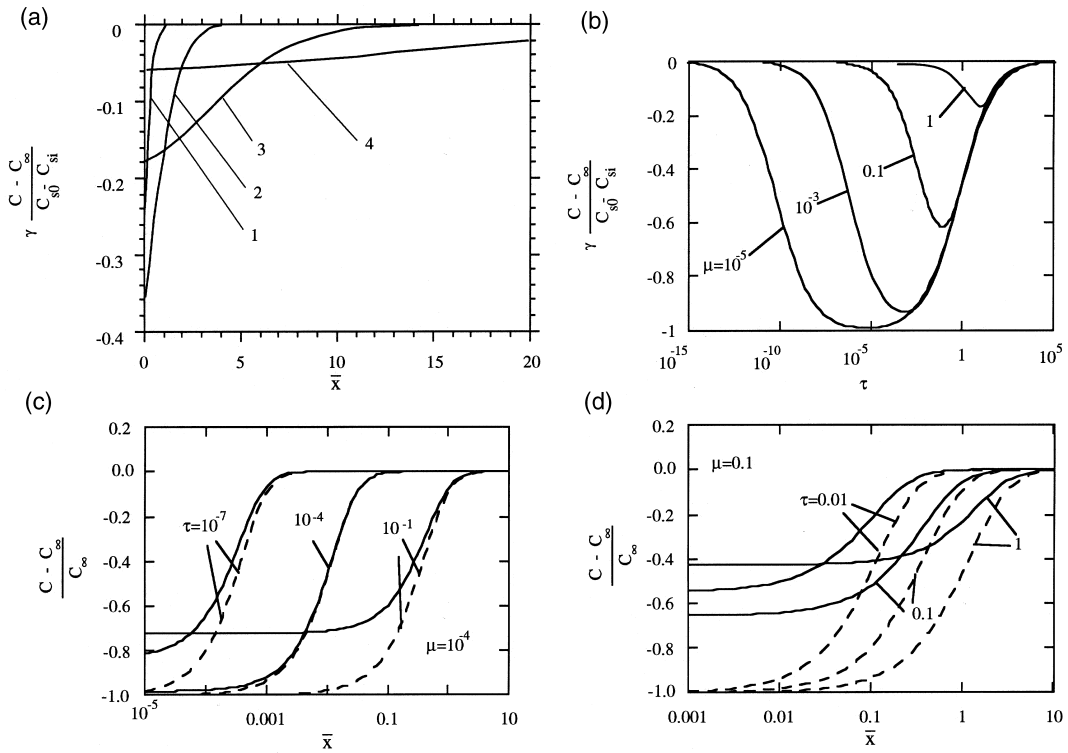

Fig. 4. The evolution of bulk impurities' concentration. (a) $\mu = 1$; 1: $\tau = 0.1$; 2: $\tau = 1.0$; 3: $\tau = 10$; 4: $\tau = 100$. (b) $\bar{x} = 0$; (c) comparison with Crank's expression. $\mu = 10^{-4}$. Solid lines: reaction–diffusion model. Dashed lines: Crank's solution; (d) comparison with Crank's expression. $\mu = 10^{-1}$. Solid lines: reaction–diffusion model. Dashed lines: Crank's solution.

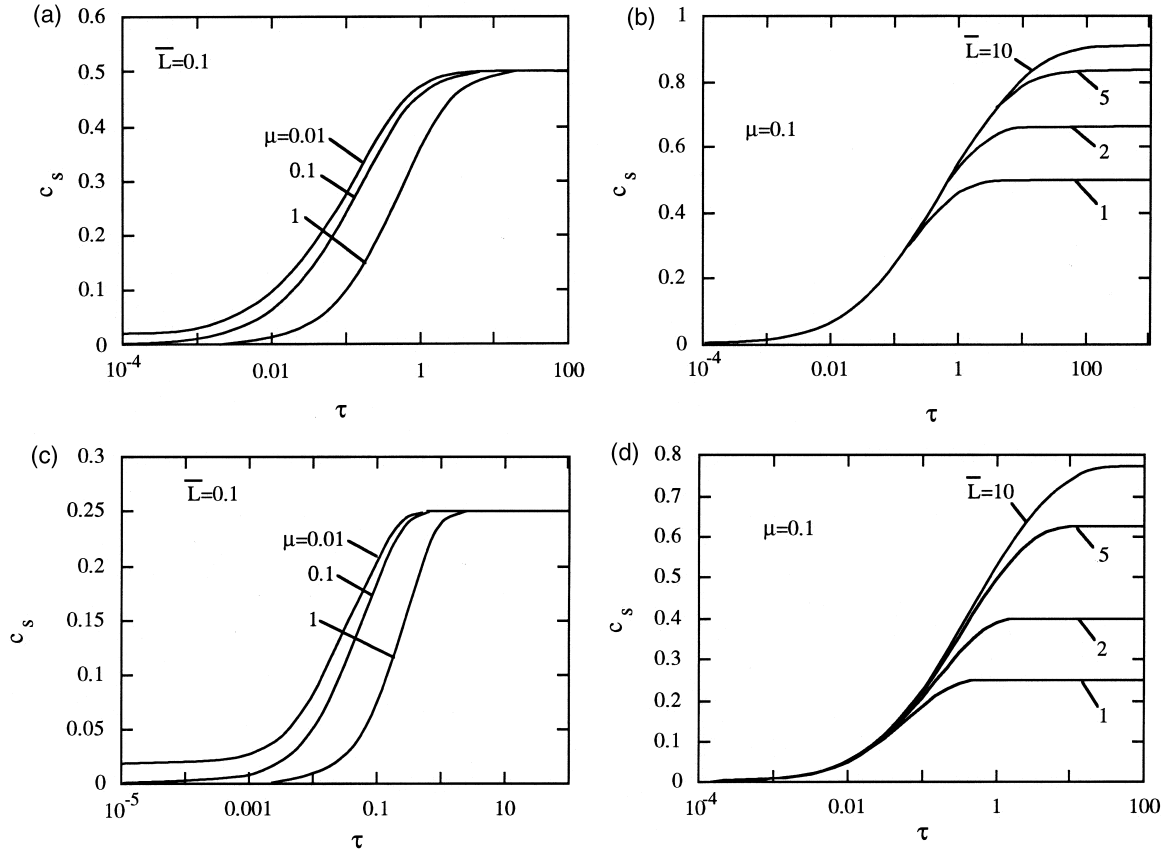

Fig. 5. Influence of the grain shape and size on the segregation kinetics. (a,b) Planar grain; (c,d) spherical grain.

Fig. 6 illustrates the effect of the nondimensional pore radius $\bar{a} = a/\delta_*$ on the rate of segregation of impurities on the surface of a cylindrical or spherical cavity. The influence of the pore curvature on the segregation kinetics is negligible at the early stage of the process, when only the impurities molecules nearest to the surface are involved in the segregation process. During this stage the surface may be considered as planar. The C_s vs. t curve has the same form as it does in the case of semi-infinite space. As the segregation process evolves, the distribution of the impurities concentration in the bulk increasingly influences the segregation kinetics, and the curves corresponding to finite pore radii, deviate from the planar solution.

One can see that the smaller the cavity, the faster the segregation process (see Fig. 6). For very small pores ($\bar{a} \to 0$), the process rate is maximal and entirely determined by the surface reaction rate (see Eq. (3)). For relatively large pores ($\bar{a} \gg 1$), the influence of the surface curvature is negligible, Eqs. (22)–(24) can be applied for the segregation kinetics analysis (as in the case of planar semi-infinite space).

4. Discussion

In several works [6,9], it was found that the $C_s(t)$ curve is likely to obey the $\sqrt{t}$ law at small times, as suggested by Eq. (2) [6]. Our model yields a linear $C_s(t)$ dependence at small times ($c_s = \mu\tau$). However, for small μ this region is very short, and the beginning of the segregation curve looks like $\sqrt{t}$. When the enrichment factor is small (weak segregation), a deviation from the $\sqrt{t}$ law has been observed [16–18]. It is seen from our model that in this case γ is also small, μ is large, and the linear region of the $C_s(t)$ curve is long, which brings about a deviation from the square root law.

Another case, in which the reaction and diffusion portions of the segregation curve can be identified, is the kinetics of segregation on small pores ($\bar{a} \ll 1$). For $\bar{a} \ll 1$ the segregation kinetics is at least partly reaction-controlled, even though the segregation to the planar surface in the same system seems to be entirely diffusion-controlled. In this case all the pure diffusion models for segregation kinetics cannot predict the

maximal rate of surface enrichment and yield infinite enrichment rate in the limit $\bar{a}\to\infty$. Our model is, therefore adequate for describing the segregation kinetics on small pores normally present in grain boundaries.

In our model a linear form of boundary condition (7) has been employed via Eq. (10). The applicability limit of this approximation has the form

$$\left|\frac{C^{\,\mathrm{eq}}_{\mathrm{appr}}(C_s)-C^{\,\mathrm{eq}}(C^{\,s})}{C^{\,\mathrm{eq}}(C_s)}\right|\ll 1, \tag{33}$$

where C_s is the current surface concentration. Condition (33) holds when C_s is close to the equilibrium value (final stage of time evolution). If (33) already holds for $C_s = C_{si}$, approximation (10) is valid during the entire process. It is easy to show that (33) is equivalent to the condition

$$\frac{|C_{si}-C_{s0}|}{1-C_{s0}}\ll 1, \tag{34}$$

which means that the linear approximation of boundary condition (7) is strictly valid as long as the initial surface concentration of segregated substance does not differ significantly from the equilibrium concentration.

Otherwise, if Eqs. (33) and (34) do not hold and one is interested in the early stages of the segregation process, Eq. (7) can be linearized near the initial surface concentration:

$$C^{\,\mathrm{eq}}_{\mathrm{appr}} = C_i + \frac{C_s - C_{si}}{\gamma_i}, \tag{35}$$

where

$$C_i = C^{\,\mathrm{eq}}(C_{si}, T), \tag{36}$$

$$\frac{1}{\gamma_i} = \left(\frac{\partial C^{\,\mathrm{eq}}}{\partial C_s}\right)_{C_{si},\,T}. \tag{37}$$

When the entire $C_s(t)$ curve is to be calculated and (33) does not hold for $C_s = C_{si}$, one should solve numerically set of Eqs. (5)–(9) without employing linearizations (10) and (35).

Strictly speaking, condition (7) may also become invalid far from the equilibrium, when Eqs. (33) and (34) do not hold. Generally, the rate of change of C_s should be described by a function of $(C)_{x=0}$, depending on a parameter $C^{\,\mathrm{eq}}(C_s, T)$:

$$\frac{\mathrm{d}C_s}{\mathrm{d}\tau} = F\left\{(C)_{x=0},\, C^{\,\mathrm{eq}}(C_s, T)\right\}. \tag{38}$$

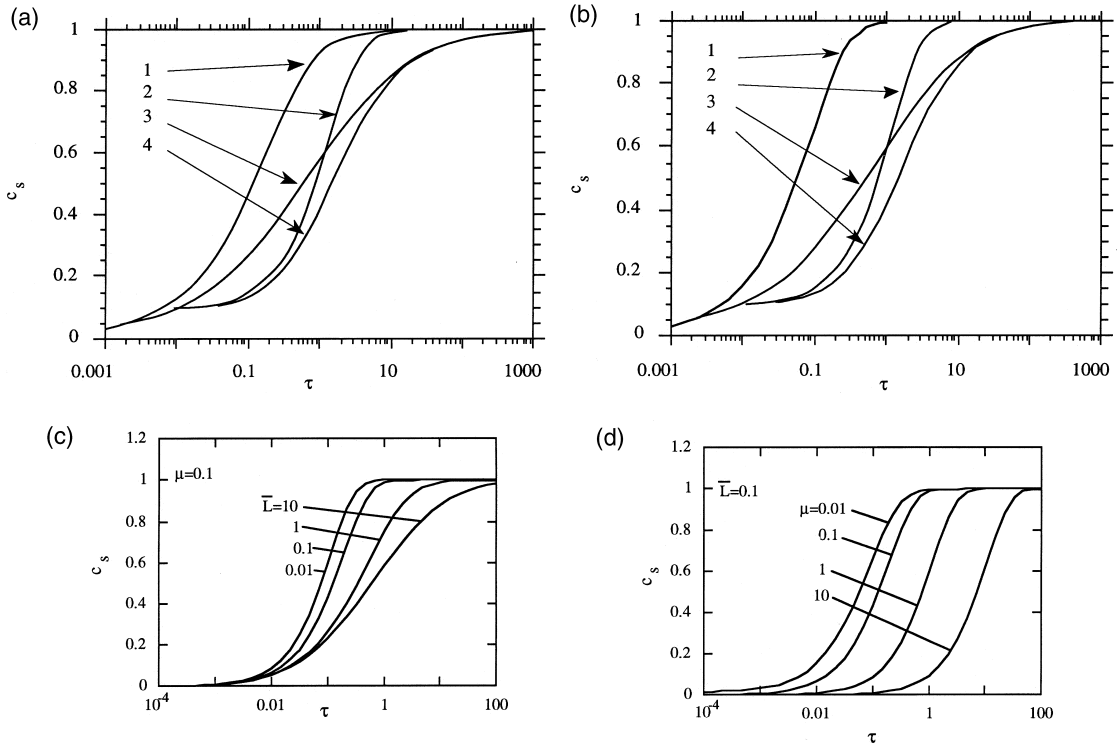

Fig. 6. The pore shape and size on the segregation kinetics. (a,b) Cylindrical pore; (c,d) spherical pore.

The specific form of this function depends on the system bulk material — segregated substance and can be determined experimentally. Since the surface concentration of impurities becomes constant at equilibrium, the value of the function $F = 0$ when $(C)_{x=0} = C^{eq}(C_s, T)$. Therefore, function F can be expanded into the Taylor series around $C^{eq}(C_s, T)$ in the following form:

$$F\{(C)_{x=0}, C^{eq}(C_s, T)\} = F'\{(C)_{x=0} - C^{eq}(C_s, T)\} + \frac{1}{2}F''\{(C)_{x=0} - C^{eq}(C_s, T)\}^2 + \ldots \quad (39)$$

where F' and F'' are the derivatives of F. In condition (7) we take only the first term of this expansion. Evaluation of the correction to the solution by accounting for the higher-order terms in expansion (39) lies beyond the scope of the present paper. The fact of mere existence of systems, in which surface segregation kinetics can be described by Eq. (3) [11–13,6] proves that the function F may be considered linear, and condition (7) is valid even far from equilibrium.

Below, we use our reaction–diffusion model for analysis of various experimental data on surface segregation kinetics, available from the literature [27,28]. Most of the results analyzed refer to segregation of solute molecules on surfaces of single metal crystals. Some of the presented data are also compared with McLeans' solution [Eq. (26)] (for $T = 900$ K see Fig. 7a, $T = 450$°C, Fig. 7b).

The parameters μ and $t_{segr} = \delta_*^2/D$ are calculated by the least square method to best fit the experimental data. The experimental points together with the theoretical curves described by Eqs. (22)–(24) are shown in

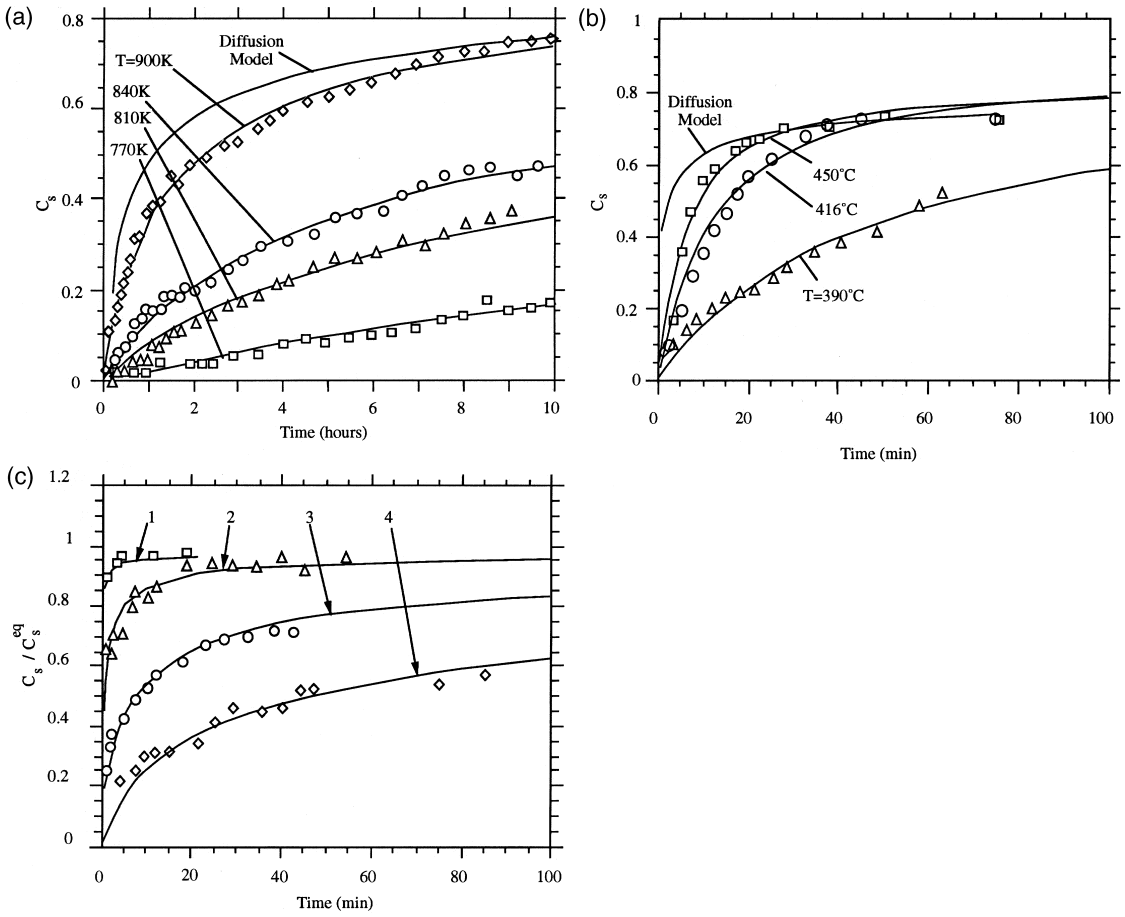

Fig. 7. (a) Comparison between experimental data on kinetics of sulfur segregation in iron [27] and results of calculations by reaction–diffusion model (at all temperatures) and by McLeans' model ($T = 900$ K). Experimental results: rhombuses: $T = 900$ K; circles: $T = 840$ K; triangles: $T = 810$ K; squares: $T = 770$ K. (b) Comparison between experimental data on kinetics of silver segregation on copper [28] and results of calculations by reaction–diffusion model (at all temperatures) and by McLeans' model ($T = 450$°C). Experimental results: squares: $T = 450$°C; circles: $T = 416$°C; triangles: $T = 390$°C.

Table 1
Parameters controlling the kinetics of sulfur segregation in iron [27]

	T (K)	D (m^2/s)	μ	t_{segr} (h)	δ_* (nm)	K (m/s)
1	900	1.911×10^{-21}	0.889	1.30	299.6	7.174×10^{-11}
2	840	5.912×10^{-19}	1.701	4.03	92.65	3.753×10^{-12}
3	810	9.208×10^{-20}	0.600	18.00	77.25	1.986×10^{-12}
4	770	6.745×10^{-21}	0.600	55.00	36.54	3.076×10^{-13}

Fig. 7. The surface crystallographic orientation for each set of experimental data is fixed. For example, Fig. 7b depicts the data on segregation kinetics of the Ag to the (111) Cu surface. Militzer et al. [27] reported only the relative Auger peak ratios for segregation of S on the iron surface. Since it was not possible to derive the exact surface coverages, a one-to-one relation has been used as a first approximation. We expect that this could reduce the accuracy of determination of μ and t_{segr} in this specific case. It is clearly seen that experimental results are satisfactorily correlated by the computed curves. Eqs. (14c) and (20) relate the material parameters K and δ_* to the parameters μ and t_{segr}. Thus, experimental data on the kinetics of segregation may also be used to determine these material parameters. Tables 1 and 2 contain the nondimensional adjustable parameters μ and t_{segr} and the segregation length δ_* and the surface reaction coefficient K, calculated on their basis. The diffusion coefficients were taken from the reference data.

Eugene et al. [28] discuss their experimental data in terms of two-dimensional phase transition at the surface. In this case, the role of surface reaction is very important. The relatively large values of μ calculated using their data for the kinetics of silver segregation on copper (see Table 2) can implicitly confirm this conclusion.

In the following we discuss the difference between the differential enrichment factor γ, appearing in Eq. (10), and conventional enrichment factor α [6]. Consider, for example, S segregation in Fe at 900 K, when the Si segregation can be ignored [27]. Assume one monolayer enrichment of S at the surface, which suggests $C_\infty \exp(E_{segr}/RT) \gg 1$, or, for $C_\infty = 1.7e-5$, $E_{segr} \gg 80$ kJ/mol K. Then the actual enrichment coefficient will be $\alpha = 1/C_\infty = 58{,}823$. From the fit value $\delta_* = 299.6$ nm and $\delta = 0.143$ nm for (100) surface one can derive $\gamma = 2095$. If one attempts to identify γ with α, one arrives at a surprising conclusion that the equilibrium surface coverage must be 0.03 monolayers, which is too small for the observed Auger signal. However, one should note that the differential enrichment factor, γ, can generally be less than α. Using the above value of $\gamma = 2095$, we can use Eq. (13) to derive the segregation energy

$$E_{segr} = RT \ln \frac{\gamma}{C_\infty^2} = 221.6 \text{ kJ/mol K}, \tag{40}$$

which is not far from the reported value 190 kJ/mol [29].

Fig. 8a presents the Arrhenius plots for the surface reaction coefficient K for two sets of data. For calculation of the time variation of surface concentration at intermediate temperatures, the temperature dependencies of K and δ_* are needed. For this purpose we correlated $K(T)$ by the equation $K = K_0 \exp(-Q_K/RT)$ with $Q_K = 236.37$ kJ/mol, $K_0 = 3.01 \times 10^3$ m/s for sulfur segregation in the Fe–6at.%Si system (Fig. 7a, Table 1), $Q_K = 126.6$ kJ/mol, $K_0 = 3.19 \times 10^{-2}$ m/s for silver segregation on the surface of copper (Fig. 7b, Table 2). The Arrhenius behavior of K is the consequence of the fact that K expresses the mobility of impurity atoms relative to bulk-surface transition and it is expected to exhibit the behavior, similar to that of the diffusion coefficient.

Fig. 8b presents the Arrhenius plots for the segregation length δ_*. This quantity characterizes the length scale on which the volume concentration of impurities is affected by the change of their surface concentration. One can see that δ_* generally exhibits an Arrhenius behavior. In the case of sulfur segregation in the Fe–6at.%Si system the segregation length δ_* can be calculated as $\delta_* = \delta_{*0} \exp(-Q_\delta/RT)$ with $Q_\delta = 90.61$ kJ/mol, $\delta_{*0} = 4.95 \times 10^7$nm. For silver segregation on the surface of copper, δ_* is almost constant. One may be tempted to express this parameter via the surface layer thickness δ and parameter γ. However, parameter γ is very sensitive to the accuracy of determination of the segregation isotherm. This parameter depends in a complicated manner on the material temperature and on the concentration of other impurities present in the

Table 2
Parameters controlling the kinetics of silver segregation in copper [28]

	T (°C)	D (m^2/s)	μ	t_{segr} (min)	δ_* (nm)	K (m/s)
1	450	5.179×10^{-19}	2.755	2.180	8.200	2.284×10^{-11}
2	416	1.0471×10^{-19}	2.020	5.010	5.610	9.234×10^{-12}
3	390	2.761×10^{-20}	0.991	40.592	8.200	3.398×10^{-12}

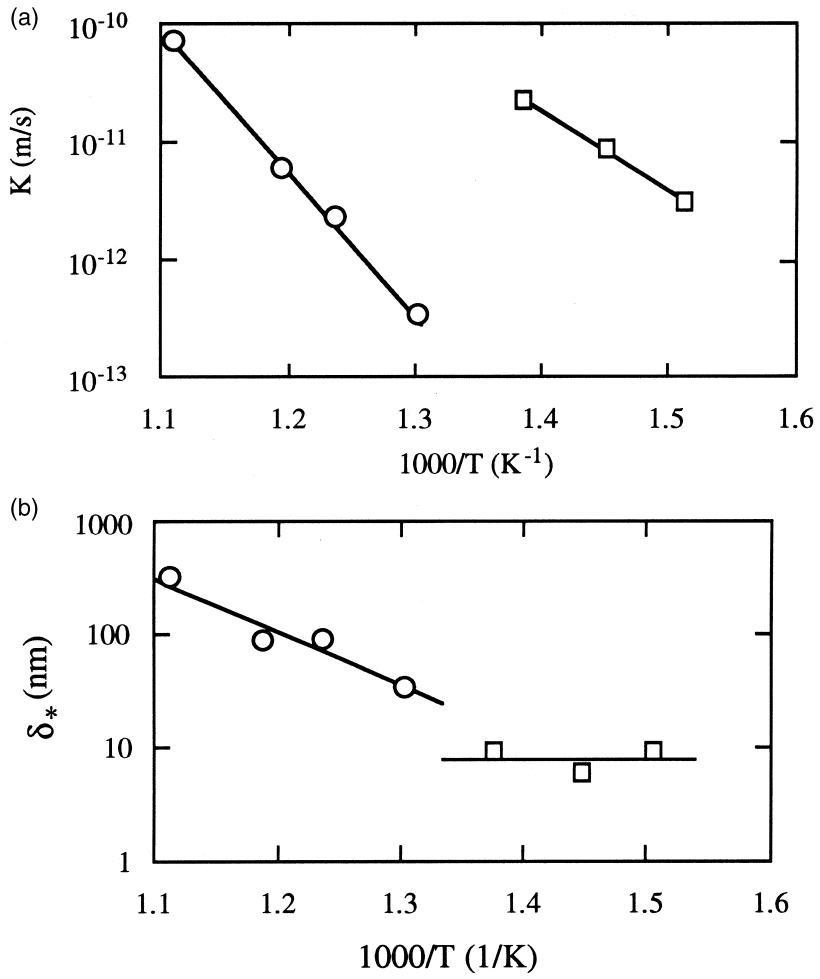

Fig. 8. (a) Arrhenius plot for K. (b) The Arrhenius plot for δ_*. Circles: data taken from Table 1; squares: data taken from Table 2.

material and their segregation energies (multicomponent segregation, see [25]). The thickness of the surface layer may also vary with temperature for certain systems [30,31].

Obviously, not every data set can be used for determination of the kinetic parameters. For example, the data for Si segregation in Fe–3wt.%Si collected by de Rugy and Viefhaus [9] have been described by Crank's expression (2) almost up to the equilibrium. In terms of our model parameters, we can conclude from the analysis of these data that in these conditions $\mu < 0.1$, or $K > 0.1D/\delta_*$. None of the models discussed here can be used for determination of kinetic parameters in the cases of surface reaction of higher orders, e.g. as described in Bezuidenhout et al. [1].

One can use our model in combination with Arrhenius plots in Fig. 8a and b to predict surface segregation rate at different temperatures. Indeed, one can fit Eqs. (22)–(24) to several segregation curves for a certain system, measured at different temperatures, to calculate the activation energies and preexponential multipliers for $K(T)$ and $\delta_*(T)$-dependencies. These parameters may be used to extrapolate K and δ_* for other temperatures and predict the corresponding segregation kinetics curves. The derived parameters allow to predict the evolution of the bulk concentration within the material, and also to qualify the influence of the shapes of grains and pores on the intergranular segregation kinetics.

5. Conclusions

A theoretical model describing the segregation kinetics is developed, accounting for bulk diffusion of impurities and their segregation. At short times ($t \ll \delta_*/K$), or for $D \gg \delta_* K$ this model reduces to reaction rate limited model [6]. At long times

($t \gg \delta_*^2/D$), or for $D \ll \delta_* K$ the segregation kinetics can be described by McLean's model with α substituted by γ.

The effect of grain size, L, is established by the parameter L/δ_*. When $L \gg \delta_*$ the grain size may be considered as infinite.

The pore size, a, affects the segregation process when $a = O(\delta_*)$. When $a \gg \delta_*$ the pore may be considered as plane surface. When $a \ll \delta_*$, the pore size also does not affect the segregation process. In this case, C_s is reaction–controlled (changes at the time scale δ_*/K) and given by Eq. (25).

The predictions of the reaction–diffusion model agree well with the experimental data on segregation kinetics. The comparison between the results of calculations and experimental data allows to determine the physical parameters, controlling the segregation kinetics, namely, K and δ_*. These parameters were found to exhibit the Arrhenius-like temperature behavior. These parameters can be used for prediction of the $C_s(t)$ curves for various thermal regimes and intergranular geometries.

Estimation of validity limits of the linearized reaction–diffusion model has been made. When the linearization assumed in Eqs. (10) and (35) is invalid, the set of nonlinear Eqs. (5)–(9) should be solved.

Appendix A. Solutions for surface concentration time variation for various geometries

In this Appendix, the Laplace images of the bulk and surface concentrations evolution are presented. The Laplace image of bulk concentration is denoted by $\hat{c}(\bar{x}, s)$ for Cartesian geometry or $\hat{c}(\bar{r}, s)$ for cylindrical or spherical geometries and the Laplace image of the surface concentration is $\hat{c}_s(s)$, where s is the Laplace transform variable.

In the case of *infinite slab*, the Laplace image of the concentration field in the bulk takes the form

$$\hat{c}(\bar{x}, s) = -\frac{1}{\gamma}\left\{\frac{\exp\left[(\bar{L}-\bar{x})\sqrt{s}\right] + \exp\left[(\bar{x}-\bar{L})\sqrt{s}\right]}{\exp\left(\bar{L}\sqrt{s}\right) - \exp\left(-\bar{L}\sqrt{s}\right)} \cdot \frac{1}{\sqrt{s}\left(\mu s + \varphi(s)\sqrt{s}+1\right)}\right\} \tag{A1}$$

and the image of surface concentration variation is

$$\hat{c}_s(s) = \frac{1}{s\left(\mu s + \varphi(s)\sqrt{s}+1\right)}, \tag{A2}$$

where

$$\varphi(s) = \coth\left(\bar{L}\sqrt{s}\right). \tag{A3}$$

An alternative geometry for analyzing the influence of grain size upon the segregation kinetics is an *infinite cylinder* with radius L. In this case, Eq. (5) must be written in cylindrical coordinates. Eq. (5) holds for $0 = r = L$, and the boundary conditions (6) and (7) hold at the surface $r = L$.

The Laplace image of the bulk concentration of impurities is described by

$$\hat{c}(\bar{r}, s) = -\frac{1}{\gamma}\frac{I_0\left(\bar{r}\sqrt{s}\right)\varphi(s)}{\sqrt{s}\left(\mu s + \varphi(s)\sqrt{s}+1\right)}, \tag{A4}$$

and the image of surface concentration is described by (A2) with

$$\varphi(s) = \frac{I_0\left(\bar{L}\sqrt{s}\right)}{I_1\left(\bar{L}\sqrt{s}\right)} \tag{A5}$$

where I_0 and I_1 are the modified Bessel functions of the first kind. This solution has limting form $C_s \to C_{si} + (C_{s0} - C_{si})(1 + 2/\bar{L})^{-1}$ as $\tau \to \infty$.

In the model of *spherical grain*, the governing equations and boundary conditions must be modified for the spherical coordinate system. Their solution in the Laplace transform domain can be written down as:

$$\hat{c}(\bar{r}, s) = -\frac{1}{\gamma}\frac{\sinh\left(\bar{r}\sqrt{s}\right)}{\bar{r}\sqrt{s}}\frac{\varphi(s)}{\sqrt{s}\left(\mu s + \varphi(s)\sqrt{s}+1\right)}, \tag{A6}$$

while the surface concentration can be described by (A2). In the case of spherical grain

$$\varphi(s) = \frac{\bar{L}\sqrt{s}}{\bar{L}\sqrt{s}\coth\left(\bar{L}\sqrt{s}\right) - 1} \tag{A7}$$

The solution has the limiting form $C_s \to C_{si} + (C_{s0} - C_{si})(1 + 3/\bar{L})^{-1}$ as $\tau \to \infty$.

In the case of *cylindrical pore* the diffusion equation will be solved in cylindrical coordinates in the domain $r \le a$. Boundary conditions (6) and (7) hold at the pore surface $r = a$. Then the bulk concentration of impurities can be calculated from

$$\hat{c}(\bar{r}, s) = -\frac{1}{\gamma}\frac{K_0\left(\bar{r}\sqrt{s}\right)\varphi(s)}{\sqrt{s}\left(\mu s + \varphi(s)\sqrt{s}+1\right)} \tag{A8}$$

The surface concentration can be calculated from (A2) with

$$\varphi(s) = \frac{K_0\left(\bar{a}\sqrt{s}\right)}{K_1\left(\bar{a}\sqrt{s}\right)} \tag{A9}$$

where K_0 and K_1 are the modified Bessel functions of the second kind. It can be shown that for $\bar{a} \to \infty$, $\varphi(s) \equiv 1$, and the solution for surface concentration history reduces to (22), valid for semi-infinite case. If, conversely, the pore is very small, $\varphi(s) \equiv 0$, and the

time variation of surface concentration can be described by Eq. (25).

In the case of the *spherical pore* the diffusion equation is solved in spherical coordinates in the domain $r \geq a$ with the surface described by $r = a$.

The solution of this problem in the Laplace's domain is

$$\hat{c}(\bar{r}, s) = -\frac{1}{\gamma}\frac{\exp\left(-\bar{r}\sqrt{s}\right)}{\bar{r}\sqrt{s}}\frac{\varphi(s)}{\sqrt{s}\left(\mu s + \varphi(s)\sqrt{s}+1\right)}, \quad \text{(A10)}$$

$$\varphi(s) = \frac{\bar{a}\sqrt{s}}{\bar{a}\sqrt{s}+1}, \quad \text{(A11)}$$

and the surface concentration can be described by (A2).

In the cases when the *near-surface diffusion* differs significantly from the bulk diffusion, the concentration distribution within the material is described by

$$\hat{c}(\bar{x}, s) = \frac{1}{\gamma}\Theta_1(s, \bar{x})\frac{\varphi(s)}{\sqrt{s}\left(\mu s + \varphi(s)\sqrt{s}+1\right)}, \quad 0 \leq x \leq b. \quad \text{(A12)}$$

$$\hat{c}(\bar{x}, s) = \frac{1}{\gamma}\Theta_2(s, \bar{x})\frac{\varphi(s)}{\sqrt{s}\left(\mu s + \varphi(s)\sqrt{s}+1\right)}, \quad x > b. \quad \text{(A13)}$$

where

$$\Theta_1(s, \bar{x}) = \sigma\frac{\exp\left(-\bar{x}\sigma\sqrt{s}\right) - \exp\left(\bar{x}\sigma\sqrt{s}\right)\frac{1-\sigma}{1+\sigma}\exp\left(-2\bar{b}\sigma\sqrt{s}\right)}{1+\frac{1-\sigma}{1+\sigma}\exp\left(-2\bar{b}\sigma\sqrt{s}\right)} \quad \text{(A14)}$$

$$\Theta_2(s, \bar{x}) = \frac{2\sigma\exp\left(-\bar{x}\sqrt{s}\right)}{(1+\sigma)\exp\left[-\bar{b}\sqrt{s}(1-\sigma)\right] - (1-\sigma)\exp\left[-\bar{b}\sqrt{s}(1+\sigma)\right]} \quad \text{(A15)}$$

The surface concentration kinetics is described by (A2) with

$$\varphi(s) = \sigma\frac{1-\frac{1-\sigma}{1+\sigma}\exp\left(-2\bar{b}\sigma\sqrt{s}\right)}{1+\frac{1-\sigma}{1+\sigma}\exp\left(-2\bar{b}\sigma\sqrt{s}\right)} \quad \text{(A16)}$$

The above Laplace images can be inverted with the help of the known analytical methods. The resulting solutions can be obtained in the form of infinite series. We, however, inverted the images numerically using the NAG software on TX work station.

References

[1] D. McLean, Grain Boundaries in Metals, Oxford University Press, Oxford, 1957.

[2] W.D. Kingery, H.K. Bowen, D.R. Uhlmann, Introduction to Ceramics, Wiley, New York, 1976.

[3] T. Gambaryan, E.Ya. Litovsky, M. Shapiro, Influence of segregation-diffusions processes on the effective thermal conductivity of porous ceramics, Int. Jour. Heat and Mass Trans. 36 (17) (1993) 4123–4131.

[4] T. Gambaryan-Roisman, E.Ya. Litovsky, M. Shapiro, A. Shavit, Effect of surface segregation kinetics on the effective thermal conductivity of porous ceramics, Int. Jour. of Heat and Mass Trans. 39 (8) (1996) 1687–1695.

[5] G. Luckman, Studies of surface segregation kinetics by Auger electron spectroscopy, in: C.L. Briant, R.P. Messmer (Eds.), Auger Electron Spectroscopy, Academic Press, Boston, 1988.

[6] J. du Plessis, Surface Segregation, Sci-Tech Publications, Vaduz, 1990.

[7] C. Lea, M.P. Seah, Kinetics of surface segregation, Philosophical Magazine 35 (1) (1977) 213–228.

[8] J. Crank, The Mathematics of Diffusion, Clarendon Press, Oxford, 1975.

[9] H. de Rugy, H. Viefhaus, Surface segregation of Si on Fe single crystal surfaces and interaction with carbon, Surface Science 173 (1986) 418–438.

[10] G. Rollands, D.P. Woodruf, Phil. Mag. A40 (1979) 459.

[11] K.J. Rawlings, S.D. Folias, B.J. Hopkins, Surface Science 109 (1981) 513.

[12] R. Sau, J.B. Hudson, J. Vac. Sci. Technol. 16 (1986) 1554.

[13] J. du Plessis, F. Bezuidenhout, G.N. van Wyk, Surface Science 177 (1986) 207.

[14] J. du Plessis, G.N. van Wyk, A model for surface segregation in multi-component alloys — Part III: the kinetics of surface segregation in a binary alloy, J. Phys. Chem. Solids 50 (N3) (1989) 237–245.

[15] E. Litovsky, T. Gambaryan-Roisman, M. Shapiro, A. Shavit, Heat transfer mechanisms governing thermal conductivity of porous ceramic materials, in: Trends in Heat, Mass and Momentum Transfer, Research Trends, India, 1997, pp. 147–167.

[16] S. Kristyan, J. Giber, Diffusion to the surface in case of weak segregation of binary alloys, Surface Science 224 (1989) 476–488.

[17] J. du Plessis, E. Taglauer, The kinetics of weak surface segregation, Surface Science 260 (1992) 355–360.

[18] J. du Plessis, P.E. Viljoen, Kinetics of the weak surface segregation of Si in an Fe–10at.%Si single crystal, Surface Science Letters 276 (1992) L7.

[19] F. Bezuidenhout, J. du Plessis, P.E. Viljoen, The segregation of carbon to the (110) surface of a Fe–10at.%Si single crystal, Surface Science 171 (1986) 392–399.

[20] O.L.J. Gijzeman, F.C. Schouten, G.A. Bootsma, Surface Science 109 (1978) 513.

[21] Shapiro, M.H., Brenner, D., Guell, Accumulation and transport of Brownian particles at solid surfaces: aerosol

and hydrosol deposition processes, J. Colloid and Interface Sci. 136 (2) (1990) 552–573.
[22] V.G. Levich, Physicochemical Hydrodynamics, Prentice-Hall, Englewood Cliffs, NJ, 1962.
[23] P. Lejček, A.V. Krajnikov, Yu.N. Ivashchenko, J. Adámek, Anisotropy of interfacial segregation: grain boundaries and free surfaces, Surface Science 269/270 (1992) 1147–1151.
[24] A. Senhaji, G. Tréglia, B. Legrand, N.T. Barrett, C. Gulliot, B. Vilette, Is the segregation–dissolution kinetics driven by a surface local equilibrium? An answer via the kinetic tight-binding ising model, Surface Science 274 (1992) 297–305.
[25] M. Guttman, D. McLean, Grain boundary segregation in multicomponent systems, in: W.C. Johnson, J.M. Blakely (Eds.), Interfacial Segregation, Am. Soc. for Metals, Metals Park, OH, 1979, pp. 261–348.
[26] M. Polak, M. Talianker, R. Arkush, Anisotropy of equilibrium surface segregation in Ni–9%Al, Surface Science 273 (1992) 363–371.
[27] M. Militzer, Yu.N. Ivashchenko, A.V. Krajnikov, P. Lejek, J. Wieting, S.A. Firstov, Surface Science 261 (1992) 267–274.
[28] J. Eugne, B. Aufray, F. Caban, Equilibrium of segregation in Au/Cu: influence of the orientation and temperature, Surface Science 27 (1992) 372–380.
[29] M.M. Eisl, B.M. Reichl, H. Stö, Depletion effects in surface segregation on sulfur from polycrystalline high-purity α-iron, Surface Science 70/71 (1993) 137–141.
[30] Y. Ikuma, W. Komatsu, The surface layer thickness and the near-surface diffusion of oxygen in metal oxides, in: Materials Science Forum, vol. 29, Trans Tech Publications, Switzerland, 1988, pp. 119–218.
[31] J. Nowotny, Certain aspects of segregation in oxide ceramic materials, in: Materials Science Forum, 29, Trans Tech Publications, Switzerland, 1988, pp. 99–126.